

Multinuclear NMR Studies on Lewis Acid–Lewis Base Interactions between Bis(pentafluorophenyl)borinic Acid and Uranyl β -Diketonato Complexes in Toluene

Naomi Miyamoto, Yasuhisa Ikeda, and Takehiko Tsukahara*

Cite This: *Inorg. Chem.* 2020, 59, 11347–11356

Read Online

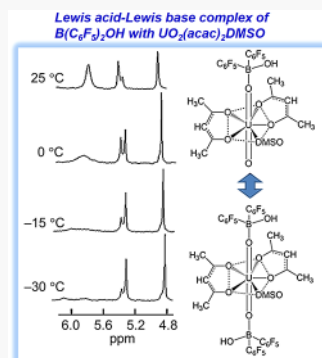
ACCESS |

Metrics & More

Article Recommendations

Supporting Information

ABSTRACT: In order to examine the possibility of Lewis acid–Lewis base (LA–LB) interactions between the boron atom of $\text{B}(\text{C}_6\text{F}_5)_2\text{OH}$ and the oxo groups (“yl” oxygen atoms) of uranyl β -diketonato complexes, we have measured the ^1H , ^{11}B , ^{17}O , ^{19}F NMR and IR spectra of toluene solutions containing β -diketonato complexes $[\text{UO}_2(\text{acac})_2\text{DMSO}]$ or $[\text{UO}_2(\text{dfh})_2\text{DMSO}]$, where acac = 2,4-pentanedionate, dfh = 1,1,1,2,2,6,6,7,7,7-decafluoroheptane-3,5-dionate, and DMSO = dimethyl sulfoxide] and $\text{B}(\text{C}_6\text{F}_5)_2\text{OH}$. ^{11}B and ^{17}O NMR spectra of solutions containing $[\text{UO}_2(\text{dfh})_2\text{DMSO}]$ and $\text{B}(\text{C}_6\text{F}_5)_2\text{OH}$ showed no change in their chemical shifts regardless of the $[\text{B}(\text{C}_6\text{F}_5)_2\text{OH}]/[\text{UO}_2(\text{dfh})_2\text{DMSO}]$ ratio. This indicates that there were no apparent interactions between $\text{B}(\text{C}_6\text{F}_5)_2\text{OH}$ and $[\text{UO}_2(\text{dfh})_2\text{DMSO}]$. On the other hand, in the corresponding NMR spectra of solutions containing $[\text{UO}_2(\text{acac})_2\text{DMSO}]$ and $\text{B}(\text{C}_6\text{F}_5)_2\text{OH}$, new signals were observed at a higher field than signals observed in the solutions containing only $\text{B}(\text{C}_6\text{F}_5)_2\text{OH}$ or $[\text{UO}_2(\text{acac})_2\text{DMSO}]$, and their intensity changed with the $[\text{B}(\text{C}_6\text{F}_5)_2\text{OH}]/[\text{UO}_2(\text{acac})_2\text{DMSO}]$ ratio. These results reveal that a complex with LA–LB interaction ($\text{B}\cdots\text{O}=\text{U}$) between the boron atom of $\text{B}(\text{C}_6\text{F}_5)_2\text{OH}$ and the “yl” oxygen atom of $[\text{UO}_2(\text{acac})_2\text{DMSO}]$ was formed. IR spectra also supported such complex formation; i.e., the asymmetric $\text{O}=\text{U}=\text{O}$ stretching band of $[\text{UO}_2(\text{acac})_2\text{DMSO}]$ was observed to shift from 897 to 810 cm^{-1} with the addition of $\text{B}(\text{C}_6\text{F}_5)_2\text{OH}$. Moreover, ^{19}F NMR spectra indicated that 1:1 and 2:1 LA–LB complexes exist in equilibrium, $\text{UO}\{\text{OB}(\text{C}_6\text{F}_5)_2\text{OH}\}(\text{acac})_2\text{DMSO} + \text{B}(\text{C}_6\text{F}_5)_2\text{OH} = \text{U}\{\text{OB}(\text{C}_6\text{F}_5)_2\text{OH}\}_2(\text{acac})_2\text{DMSO}$. The thermodynamic parameters for this equilibrium were obtained as $K = (2.5 \pm 0.6) \times 10^2 \text{ M}^{-1}$ (at 25 $^\circ\text{C}$), $\Delta H = -42.4 \pm 5.2 \text{ kJ mol}^{-1}$, and $\Delta S = -96.7 \pm 19.4 \text{ J K}^{-1} \text{ mol}^{-1}$. In ^1H NMR spectra, the signal due to $-\text{CH}$ groups of $[\text{UO}_2(\text{acac})_2\text{DMSO}]$ disappeared, and three signals due to the corresponding $-\text{CH}$ groups newly appeared with an increase in the $[\text{B}(\text{C}_6\text{F}_5)_2\text{OH}]/[\text{UO}_2(\text{acac})_2\text{DMSO}]$ ratio. From these phenomena, it is proposed that 1:1 and 2:1 LA–LB complexes having interactions between the $-\text{CH}$ groups of acac and the $-\text{OH}$ group of coordinated $\text{B}(\text{C}_6\text{F}_5)_2\text{OH}$ are formed depending on the $[\text{B}(\text{C}_6\text{F}_5)_2\text{OH}]/[\text{UO}_2(\text{acac})_2\text{DMSO}]$ ratio.



INTRODUCTION

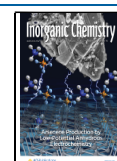
Oxo groups of the uranyl ion (UO_2^{2+}), the so-called “yl” oxygen atoms, are considered to be chemically inert because of their linear and covalent $\text{O}=\text{U}=\text{O}$ bonds in contrast to transition-metal oxo complexes (CrO_2^{2+} , MoO_2^{2+} , and WO_2^{2+}), which play roles as catalysts in chemical and biochemical oxidation processes.^{1–3} Recently, the functionalization of “yl” oxygen atoms of UO_2^{2+} has attracted much attention in the fields of environmental remediation, uranium mining, and geological disposal of nuclear wastes.^{4–10} This is because an understanding of the functionalization mechanisms provides important insights into not only reactions such as the reduction and ligand exchange of uranyl complexes but also the migration behavior of uranyl species in the environment. Several studies have clarified that the specific ligands coordinated in the equatorial plane of the UO_2^{2+} moiety allow functionalization of the “yl” oxygen atoms of UO_2^{2+} in solvents. Examples of the unique functionalization of “yl” oxygen atoms include isotopic exchange between the “yl” oxygen atoms and solvent oxygen atom,^{11–15} oxo substitution

reactions from $\text{U}=\text{O}$ to $\text{U}=\text{N}$ bonds,^{16,17} and ligand scrambling between $\text{U}=\text{O}$ bonds and hydroxides.^{18,19}

Novel uranyl complexes with high Lewis basicity have been investigated to reveal the unique reactivity of “yl” oxygen atoms in uranyl complexes.^{7,19,20} Because the Lewis basicity of the uranyl “yl” oxygen atoms enables enhancement with an increase in the electron donicity of the ligands in the equatorial plane of the uranyl moiety, the “yl” oxygen atoms can directly coordinate to Lewis acidic compounds because of Lewis acid (LA)–Lewis base (LB) interactions. Various types of uranyl complexes have been successfully synthesized and characterized by means of crystallographic and spectroscopic methods, e.g., reductive silylation of the uranyl ion,^{21–23}

Received: April 2, 2020

Published: July 30, 2020



pentavalent uranyl coordination polymers,^{24–28} uranyl–metal ion cation–cation complexes, pentavalent uranyl polymetallic assemblies involving metal ions,^{29–32} and uranyl ion with perfluoroarylborane adducts.^{33–35} These results have shown that alkali-, transition-, and rare-earth-metal ions, the uranyl cation itself, and perfluoroarylborane are suitable Lewis acidic compounds for coordination to the “yl” oxygen atoms of uranyl complexes through LA–LB interactions. Such interactions are formed in limited coordination environments and are not necessarily observed in all uranyl complexes.

Despite research efforts on the LA–LB complexes, most studies have mainly focused on the coordination structures and reactivity. Hence, the mechanisms of the LA–LB complex formations have not been fully clarified; i.e., evidence about whether the Lewis acidic compounds can directly coordinate to the Lewis basic “yl” oxygen atoms of uranyl complexes or interact with ligands in the equatorial plane of the uranyl moiety is not available. To understand them, the molecular interactions among each functional group of Lewis acidic compounds and uranyl complexes in solutions need to be explored.

Highly electrophilic perfluoroarylboranes such as tris-(pentafluorophenyl)borane [$B(C_6F_5)_3$] and bis-(pentafluorophenyl)borinic acid [$B(C_6F_5)_2OH$] are well-known to be effective Lewis acidic reagents and to form LA–LB complexes with Lewis basic uranyl complexes.^{29–31,36} In particular, $B(C_6F_5)_2OH$ is an adequate LA compound for easy treatment in various solutions because $B(C_6F_5)_3$ having higher Lewis acidity than $B(C_6F_5)_2OH$ is often destabilized because of its interaction with water in solvents and in the atmosphere.^{37,38} On the other hand, uranyl β -diketonato complexes are suitable Lewis basic compounds for examining LA–LB interactions in solutions because the Lewis basicity of their “yl” oxygen atoms can be flexibly changed by using various β -diketonates as equatorial ligands.

On the basis of the above background, we previously carried out ^{11}B and ^{19}F NMR measurements of toluene solutions containing uranyl β -diketonato complexes and $B(C_6F_5)_2OH$ because NMR spectroscopy is recognized as a helpful tool for determining the intermolecular interactions of solutes in solutions. In fact, previous NMR studies have succeeded in the characterization of structures and ligand-exchange reactions of uranyl complexes in various solvents, as well as understanding local interactions between the ligands coordinated to the uranyl moiety and solvents.^{39–50} As a result, we have succeeded in discovering the possibility of LA–LB interactions between $B(C_6F_5)_2OH$ and uranyl β -diketonato complexes.⁵¹ However, there are many indeterminate aspects about the LA–LB complexation mechanisms such how the LA–LB interactions change by the coordinating ligand species and solvent environments and what types of LA–LB complexes are formed.

Therefore, in this work, we aim to clarify the microscopic molecular interactions of functional moieties such as hydrocarbon, fluorocarbon, hydroxyl, “yl” oxygen, and boron in the uranyl complexes and $B(C_6F_5)_2OH$ and to obtain direct evidence that the Lewis acidic boron atom of $B(C_6F_5)_2OH$ can coordinate to the Lewis basic “yl” oxygen atoms of uranyl complexes. In particular, the effects of the ratios of $[B(C_6F_5)_2OH]/[uranyl\ complex]$, differences in the functional moieties, and temperature on the LA–LB complex formation were examined by means of multinuclear (1H , ^{11}B , ^{17}O , and ^{19}F) NMR measurements of toluene solutions containing

$B(C_6F_5)_2OH$ and uranyl β -diketonato complexes [$UO_2(acac)_2DMSO$ or $UO_2(dhf)_2DMSO$, where $acac = 2,4$ -pentanedionate, $dhf = 1,1,1,2,2,6,6,7,7,7$ -decafluoroheptane-3,5-dionate, and $DMSO =$ dimethyl sulfoxide]. Moreover, changes in the $U=O$ bond strength due to LA–LB interactions were directly evaluated by IR spectroscopy.

EXPERIMENTAL SECTION

Materials. 2,4-Pentanedione (Hacac), 1,1,1,2,2,6,6,7,7,7-decafluoroheptane-3,5-dione (Hdhf), and $B(C_6F_5)_3$ were purchased from Kanto Chemical Co. Inc., Matrix Scientific, and Tokyo Chemical Industry Co. Ltd., respectively, and used without further purification. Dimethyl sulfoxide (DMSO), toluene, *n*-pentane, *n*-hexane, and dichloromethane (Kanto Chemical Co. Inc.) were used after storage over 4A molecular sieves. The $UO_2(dhf)_2DMSO$ and $UO_2(acac)_2DMSO$ complexes were synthesized by the method reported in a previous paper⁵² and recrystallized from *n*-hexane/ CH_2Cl_2 . 1H and ^{19}F NMR spectra of $UO_2(dhf)_2DMSO$ and the 1H NMR spectrum of $UO_2(acac)_2DMSO$ were measured to confirm the coordination numbers of dhf, acac, and DMSO in $CDCl_3$ solvents. We found that the 1H NMR spectrum of $UO_2(acac)_2DMSO$ was consistent with that in a previous study,³⁹ and the peak area ratios of 1H and ^{19}F NMR spectra of $UO_2(dhf)_2DMSO$ were compatible with those predicted from the chemical structure. Accordingly, the uranyl complexes can be identified as complexes with two bidentate dhf or acac and one unidentate DMSO in the equatorial plane of the uranyl(VI) moiety.

Preparation of $B(C_6F_5)_2OH$. $B(C_6F_5)_2OH$ was synthesized by hydrolysis of $B(C_6F_5)_3$, as presented in previous reports.⁵³ $B(C_6F_5)_3$ (2.0 g) was dissolved in toluene (15.0 mL) and refluxed with stirring at 85 °C. After dropping water (70.0 μL , equivalent to $[B(C_6F_5)_3]$) gradually into the toluene solution containing $B(C_6F_5)_3$, part of the toluene solution was taken out every 1 h, and their ^{11}B and ^{19}F NMR spectra were measured at 25 °C to confirm the formation of $B(C_6F_5)_2OH$. Although the initial ^{11}B NMR spectrum showed one signal at 60.0 ppm, with the elapse of time, the signal intensity decreased and a new peak appeared at 40.0 ppm. After 9 h, the ^{11}B NMR signal at 60.0 ppm completely disappeared and only one signal at 40.0 ppm was observed. In ^{19}F NMR spectra, three signals due to $B(C_6F_5)_3$ were observed initially at -130.0 , -143.1 , and -161.3 ppm. After 9 h, three signals were newly detected at -133.1 , -148.2 , and -161.3 ppm. These new signals were assigned as $B(C_6F_5)_2OH$ because of their good agreement with previous reports.^{54,55} From these NMR results, it was confirmed that $B(C_6F_5)_3$ was converted to $B(C_6F_5)_2OH$. After almost 100% conversion to $B(C_6F_5)_2OH$ was achieved, toluene was removed by bubbling Ar gas. White precipitates containing $B(C_6F_5)_2OH$ and impurities were obtained. Because only $B(C_6F_5)_2OH$ in the precipitates was found to dissolve in *n*-pentane, the insoluble impurities were removed from $B(C_6F_5)_2OH$ dissolved in *n*-pentane by filtration. The filtrate containing $B(C_6F_5)_2OH$ was refined by cooling to -35 °C and refluxing for 5 h. *n*-Pentane was removed by supplying Ar gas, and finally a white powder of $B(C_6F_5)_2OH$ (0.6 g) was obtained.

Preparation of Uranyl Complexes with ^{17}O -Enriched “yl” Oxygen Atoms. ^{17}O -enriched uranyl nitrate hexahydrate [$U^{17}O_2(NO_3)_2 \cdot 6H_2O$] was prepared by irradiating UV light (hollow cathode lamp, 10 W and max. 460 nm; L233-38NB, Hamamatsu Photonics K.K.) onto the solution prepared by dissolving $UO_2(NO_3)_2 \cdot 6H_2O$ in ^{17}O -enriched water ($H_2^{17}O$ 30–40%; Cambridge Isotope Lab., Inc.) for 30 min.⁵⁶ The $U^{17}O_2(dhf)_2DMSO$ complex was synthesized according to a previous paper.⁵⁷ The CH_2Cl_2 solution containing DMSO and Hdhf was dropped into the aqueous solution, dissolving $U^{17}O_2(NO_3)_2 \cdot 6H_2O$, followed by shaking to extract $U^{17}O_2(dhf)_2DMSO$ to the CH_2Cl_2 phase. After evaporation of the CH_2Cl_2 phase, yellow precipitates were obtained and recrystallized from CH_2Cl_2 . The $U^{17}O_2(acac)_2DMSO$ complex was synthesized according to previous papers as follows.⁵² The pH of the aqueous solution with dissolved $U^{17}O_2(NO_3)_2 \cdot 6H_2O$ was adjusted to approximately 5 by adding a sodium hydroxide aqueous solution.

By shaking of the pH-adjusted aqueous solution and the CH_2Cl_2 solution containing Hacac, $\text{U}^{17}\text{O}_2(\text{acac})_2\cdot\text{H}_2\text{O}$ was extracted to the CH_2Cl_2 phase. A yellow precipitate was obtained by removing CH_2Cl_2 and dried in a vacuum desiccator with phosphorus pentoxide at 100°C for 1 day. Moreover, this precipitate was dissolved in warm DMSO, and then the DMSO solution was cooled to room temperature. As a result, orange $\text{U}^{17}\text{O}_2(\text{acac})_2\text{DMSO}$ crystals were obtained.

Apparatuses. Details of the NMR apparatus used in this study have been described in our previous paper.^{57,58} ^{11}B , ^{17}O , and ^{19}F NMR spectra were measured by using a JEOL JNM-LA300 spectrometer without spinning at 300.0, 96.3, 40.6, and 282.2 MHz, respectively; a zirconia sample tube prepared for studying the behavior of $\text{UO}_2(\text{dfh})_2\text{DMSO}$ in supercritical CO_2 was used to refer to the previous NMR data.⁵⁷ After sample solutions were placed in the zirconia sample tube, the tube was sealed with a stainless sample holder and O-ring in a glovebox filled with Ar gas. The temperature of the zirconia sample tube was controlled by the temperature controller of the NMR probe. ^{11}B and ^{17}O NMR spectra of toluene solutions were measured at 25°C . ^{19}F NMR measurements were carried out in the temperature range of -30 to $+25^\circ\text{C}$. ^1H NMR spectra were measured at temperatures in the range of -30 to 25°C using a JEOL JNM-ECX400P spectrometer at 400.0 MHz. ^{11}B NMR chemical shifts were measured without a deuterium lock reagent and determined by using an external reference of $\text{BF}_3\cdot\text{OEt}_2$ (0.0 ppm). A mixture of D_2O and 1,4-dioxane- d_8 (0.0 ppm) and that of fluorobenzene (-113.0 ppm) and benzene- d_6 were used as lock and reference solvents for ^{17}O and ^{19}F NMR measurements, respectively. Capillaries containing these solutions were inserted into the zirconia sample tube. ^1H NMR chemical shifts were referenced to toluene- d_8 (7.09 ppm). IR spectra of sample solutions were measured with a Shimadzu FTIR-8400S spectrophotometer in the range of 400 – 4000 cm^{-1} on thin liquid films between NaCl plates.

RESULTS AND DISCUSSION

^{11}B NMR Spectra of Toluene Solutions Containing $\text{B}(\text{C}_6\text{F}_5)_2\text{OH}$ and Uranyl Complexes. ^{11}B NMR spectra of toluene solutions containing $\text{B}(\text{C}_6\text{F}_5)_2\text{OH}$ $[(2.6\text{--}7.6) \times 10^{-3}\text{ M}]$, where $\text{M} = \text{mol dm}^{-3}$ were measured at 25°C . One signal due to $\text{B}(\text{C}_6\text{F}_5)_2\text{OH}$ was observed at 40.0 ppm (δ_{initial} ; Figure S1), which is consistent with that in a previous paper.⁵⁴ ^{11}B NMR spectra of toluene solutions containing $\text{B}(\text{C}_6\text{F}_5)_2\text{OH}$ $[(2.8\text{--}7.6) \times 10^{-3}\text{ M}]$ and $\text{UO}_2(\text{dfh})_2\text{DMSO}$ ($1.0 \times 10^{-3}\text{ M}$) were also measured (Figure S2). One signal was observed at 40 ppm independent of the $[\text{B}(\text{C}_6\text{F}_5)_2\text{OH}]_{\text{total}}/[\text{UO}_2(\text{dfh})_2\text{DMSO}]$ ratio, where $[\text{B}(\text{C}_6\text{F}_5)_2\text{OH}]_{\text{total}}$ expresses the total concentration of $\text{B}(\text{C}_6\text{F}_5)_2\text{OH}$ in toluene. This result indicates that there are no apparent interactions between $\text{B}(\text{C}_6\text{F}_5)_2\text{OH}$ and $\text{UO}_2(\text{dfh})_2\text{DMSO}$ in toluene.

On the other hand, when the $\text{UO}_2(\text{acac})_2\text{DMSO}$ complex ($1.0 \times 10^{-3}\text{ M}$) was added to the toluene solution containing $\text{B}(\text{C}_6\text{F}_5)_2\text{OH}$ ($1.1 \times 10^{-3}\text{ M}$), a drastic change was observed in the ^{11}B NMR spectrum (Figure 1a); i.e., the signal corresponding to δ_{initial} disappeared, and a new signal appeared at around 5.0 ppm (δ_{new}). The appearance of the δ_{new} signal suggests the interaction of the Lewis acidic boron atom of $\text{B}(\text{C}_6\text{F}_5)_2\text{OH}$ with the Lewis basic “yl” oxygen atoms of $\text{UO}_2(\text{acac})_2\text{DMSO}$ (abbreviated as the 1:1 complex) because the ^{11}B NMR signal due to $\text{B}(\text{C}_6\text{F}_5)_3$ is known to be observed at higher magnetic fields as a result of the interaction between the boron atom of $\text{B}(\text{C}_6\text{F}_5)_3$ and the oxygen atom of metal oxo complexes.^{29,59} Moreover, we measured ^{11}B NMR spectra of toluene solutions containing $\text{B}(\text{C}_6\text{F}_5)_2\text{OH}$ and $\text{UO}_2(\text{acac})_2\text{DMSO}$ with various $[\text{B}(\text{C}_6\text{F}_5)_2\text{OH}]_{\text{total}}/[\text{UO}_2(\text{acac})_2\text{DMSO}]$ ratios (Figure 1b–f). As seen from Figure 1, the δ_{initial} signal due to $\text{B}(\text{C}_6\text{F}_5)_2\text{OH}$ appears again

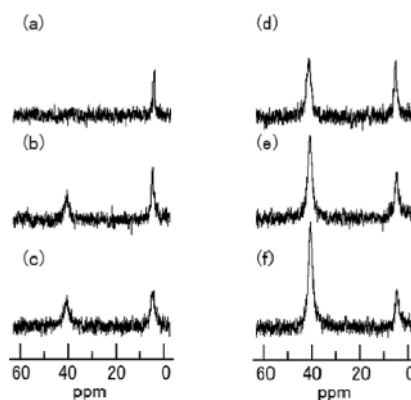


Figure 1. ^{11}B NMR spectra of toluene solutions containing $\text{B}(\text{C}_6\text{F}_5)_2\text{OH}$ and $\text{UO}_2(\text{acac})_2\text{DMSO}$ ($1.0 \times 10^{-3}\text{ M}$). $[\text{B}(\text{C}_6\text{F}_5)_2\text{OH}]_{\text{total}} = 1.1 \times 10^{-3}\text{ M}$ (a), $2.4 \times 10^{-3}\text{ M}$ (b), $3.5 \times 10^{-3}\text{ M}$ (c), $5.0 \times 10^{-3}\text{ M}$ (d), $6.5 \times 10^{-3}\text{ M}$ (e), and $7.7 \times 10^{-3}\text{ M}$ (f).

and its relative intensity to the δ_{new} peak increases with increasing $[\text{B}(\text{C}_6\text{F}_5)_2\text{OH}]_{\text{total}}$, while the chemical shifts of the δ_{new} and δ_{initial} signals are constant, independent of $[\text{B}(\text{C}_6\text{F}_5)_2\text{OH}]_{\text{total}}$. These results indicate that in the present solutions two kinds of $\text{B}(\text{C}_6\text{F}_5)_2\text{OH}$ species exist; i.e., one is free $\text{B}(\text{C}_6\text{F}_5)_2\text{OH}$, and another is $\text{B}(\text{C}_6\text{F}_5)_2\text{OH}$ interacting with $\text{UO}_2(\text{acac})_2\text{DMSO}$ (their concentrations are abbreviated as $[\text{B}]_{\text{initial}}$ and $[\text{B}]_{\text{new}}$, respectively). The $[\text{B}]_{\text{new}}$ and $[\text{B}]_{\text{initial}}$ values were evaluated from the peak areas of the δ_{new} and δ_{initial} signals obtained by line-shape analyses based on Lorentz curves. Plots of $[\text{B}]_{\text{new}}$ and $[\text{B}]_{\text{initial}}$ against $[\text{B}(\text{C}_6\text{F}_5)_2\text{OH}]_{\text{total}}$ are shown in Figure 2. In this figure, $[\text{B}]_{\text{new}}$ and $[\text{B}]_{\text{initial}}$ at

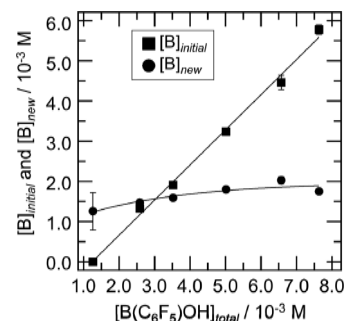


Figure 2. Plots of $[\text{B}]_{\text{initial}}$ (■) and $[\text{B}]_{\text{new}}$ (●) against $[\text{B}(\text{C}_6\text{F}_5)_2\text{OH}]_{\text{total}}$ based on the ^{11}B NMR spectra shown in Figure 1.

$[\text{B}(\text{C}_6\text{F}_5)_2\text{OH}]_{\text{total}} = 1.1 \times 10^{-3}\text{ M}$ are presented as 1.1×10^{-3} and 0.0 M , respectively, as the δ_{initial} signal is not observed, as shown in Figure 1a. As seen from Figure 2, with an increase in $[\text{B}(\text{C}_6\text{F}_5)_2\text{OH}]_{\text{total}}$, the $[\text{B}]_{\text{initial}}$ values increase linearly from 0.0 to $5.9 \times 10^{-3}\text{ M}$, while the $[\text{B}]_{\text{new}}$ values increase slightly from $1.1 \times 10^{-3}\text{ M}$ and approach a constant value of ca. $2.0 \times 10^{-3}\text{ M}$. In the present experiment, the concentration of $\text{UO}_2(\text{acac})_2\text{DMSO}$ is $1.0 \times 10^{-3}\text{ M}$ and the maximum $[\text{B}]_{\text{new}}$ value is almost $2.0 \times 10^{-3}\text{ M}$. This suggests that, under the condition $[\text{B}(\text{C}_6\text{F}_5)_2\text{OH}]_{\text{total}}/[\text{UO}_2(\text{acac})_2\text{DMSO}] \leq 1$, the 1:1 complex is formed stoichiometrically and that the complex with two $\text{B}(\text{C}_6\text{F}_5)_2\text{OH}$ molecules coordinated to two “yl” oxygen atoms of $\text{UO}_2(\text{acac})_2\text{DMSO}$ (abbreviated as the 2:1 complex) is also formed with an increase in $[\text{B}(\text{C}_6\text{F}_5)_2\text{OH}]_{\text{total}}/[\text{UO}_2(\text{acac})_2\text{DMSO}]$. However, ^{11}B NMR signals corresponding to 1:1 and 2:1 LA–LB complexes were not observed. This is considered to be due to the overlapping

of the ^{11}B NMR signals of $\text{B}(\text{C}_6\text{F}_5)_2\text{OH}$ for the 1:1 and 2:1 LA–LB complexes at the same chemical shift. Thus, in order to elucidate whether the $\text{B}(\text{C}_6\text{F}_5)_2\text{OH}$ molecule interacts directly with “yl” oxygen atoms of $\text{UO}_2(\text{acac})_2\text{DMSO}$ and the 1:1 and 2:1 complexes coexist, we tried to measure ^{17}O NMR spectra of toluene solutions containing $\text{B}(\text{C}_6\text{F}_5)_2\text{OH}$ and $\text{UO}_2(\text{dfh})_2\text{DMSO}$ or $\text{UO}_2(\text{acac})_2\text{DMSO}$.

^{17}O NMR Spectra of Toluene Solutions Containing $\text{B}(\text{C}_6\text{F}_5)_2\text{OH}$ and Uranyl Complexes. ^{17}O NMR spectra of toluene solutions containing $\text{B}(\text{C}_6\text{F}_5)_2\text{OH}$ $[(0\text{--}2.5) \times 10^{-3} \text{ M}]$ and $\text{UO}_2(\text{dfh})_2\text{DMSO}$ ($1.0 \times 10^{-3} \text{ M}$) or $\text{UO}_2(\text{acac})_2\text{DMSO}$ ($1.0 \times 10^{-3} \text{ M}$) were examined at 25°C .

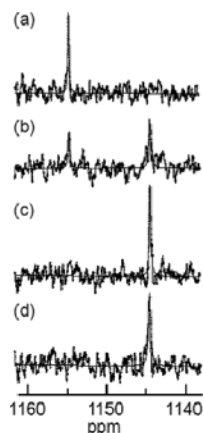


Figure 3. ^{17}O NMR spectra of toluene solutions containing $\text{B}(\text{C}_6\text{F}_5)_2\text{OH}$ and $\text{UO}_2(\text{acac})_2\text{DMSO}$ ($1.0 \times 10^{-3} \text{ M}$). $[\text{B}(\text{C}_6\text{F}_5)_2\text{OH}]_{\text{total}} = 0.0 \text{ M}$ (a), $0.5 \times 10^{-3} \text{ M}$ (b), $1.0 \times 10^{-3} \text{ M}$ (c), and $2.5 \times 10^{-3} \text{ M}$ (d).

The results are shown in Figures S3 and 3, respectively. The ^{17}O NMR signals due to $\text{U}^{17}\text{O}_2(\text{dfh})_2\text{DMSO}$ and $\text{U}^{17}\text{O}_2(\text{acac})_2\text{DMSO}$ were observed at 1160 and 1155 ppm, respectively, as shown in Figures S3a and 3, respectively. The difference in the ^{17}O NMR chemical shifts (^{17}O - δ s) between $\text{U}^{17}\text{O}_2(\text{dfh})_2\text{DMSO}$ and $\text{U}^{17}\text{O}_2(\text{acac})_2\text{DMSO}$ indicates that the ^{17}O nuclear shielding of $\text{U}^{17}\text{O}_2(\text{acac})_2\text{DMSO}$ is larger than that of $\text{U}^{17}\text{O}_2(\text{dfh})_2\text{DMSO}$ with electronegative fluorine.

In Figure S3b,c, the ^{17}O NMR signal of $\text{U}^{17}\text{O}_2(\text{dfh})_2\text{DMSO}$ is found to be observed at the same chemical shift (^{17}O - δ s = 1160 ppm) regardless of $[\text{B}(\text{C}_6\text{F}_5)_2\text{OH}]_{\text{total}}$. This indicates that the “yl” oxygen atoms of $\text{UO}_2(\text{dfh})_2\text{DMSO}$ have no interaction with $\text{B}(\text{C}_6\text{F}_5)_2\text{OH}$ and support the result derived from ^{11}B NMR measurements. On the other hand, as seen from Figure 3, in the toluene solutions containing $\text{U}^{17}\text{O}_2(\text{acac})_2\text{DMSO}$ and $\text{B}(\text{C}_6\text{F}_5)_2\text{OH}$, with increasing $[\text{B}(\text{C}_6\text{F}_5)_2\text{OH}]_{\text{total}}$, the ^{17}O NMR signal at 1155 ppm becomes small (Figure 3b) and disappears with an appearance of a new signal at 1144 ppm (Figure 3c; $[\text{B}(\text{C}_6\text{F}_5)_2\text{OH}]_{\text{total}}/[\text{UO}_2(\text{acac})_2\text{DMSO}] = 1$). Moreover, in spite of the addition of more than 2 equiv of $\text{B}(\text{C}_6\text{F}_5)_2\text{OH}$ ($2.5 \times 10^{-3} \text{ M}$) to $\text{UO}_2(\text{acac})_2\text{DMSO}$ ($1.0 \times 10^{-3} \text{ M}$) (Figure 3d), further changes in the ^{17}O NMR signals and the appearance of the ^{17}O NMR signal corresponding to free $\text{UO}_2(\text{acac})_2\text{DMSO}$ (at 1155 ppm) were not observed. These results indicate that the ^{17}O NMR signal at 1144 ppm is due to the “yl” oxygen atoms of $\text{UO}_2(\text{acac})_2\text{DMSO}$ interacting with $\text{B}(\text{C}_6\text{F}_5)_2\text{OH}$ and involves the 1:1 and 2:1 LA–LB complexes, suggesting that 1:1 and 2:1 complexes are formed under the conditions of $[\text{B}(\text{C}_6\text{F}_5)_2\text{OH}]_{\text{total}}/$

$[\text{UO}_2(\text{acac})_2\text{DMSO}] \leq 1$ and $[\text{B}(\text{C}_6\text{F}_5)_2\text{OH}]_{\text{total}}/[\text{UO}_2(\text{acac})_2\text{DMSO}] > 1$, respectively. The phenomena in ^{17}O NMR spectra are consistent with those in ^{11}B NMR measurements, in which the signals due to the 1:1 and 2:1 complexes are observed at the same chemical shift. It is noteworthy that the ^{17}O NMR signal of $\text{UO}_2(\text{acac})_2\text{DMSO}$ forming a LA–LB interaction with $\text{B}(\text{C}_6\text{F}_5)_2\text{OH}$ is observed at higher magnetic fields than that of $\text{UO}_2(\text{acac})_2\text{DMSO}$ because the “yl” oxygen atom acts as the electron donor and, hence, the ^{17}O NMR signal of the “yl” oxygen atoms is shifted to lower magnetic fields with the formation of LA–LB interactions. This opposite tendency suggests that $\text{B} \cdots \text{O}=\text{U}$ bonding due to the vacant p orbital of the boron atom and an oxygen lone pair plays an important role in the interaction between $\text{B}(\text{C}_6\text{F}_5)_2\text{OH}$ and $\text{UO}_2(\text{acac})_2\text{DMSO}$.

IR Spectra of Toluene Solutions Containing $\text{B}(\text{C}_6\text{F}_5)_2\text{OH}$ and Uranyl Complexes. If the specific LA–LB interactions are attributable to $\text{B} \cdots \text{O}=\text{U}$ bonding, the $\text{U}=\text{O}$ bonding should be reflected as changes in the bond length of $\text{U}=\text{O}$. Therefore, we carried out measurements of IR spectra. IR spectra of toluene solutions containing $\text{B}(\text{C}_6\text{F}_5)_2\text{OH}$ and $\text{UO}_2(\text{dfh})_2\text{DMSO}$ are shown in Figure 4c, with those of

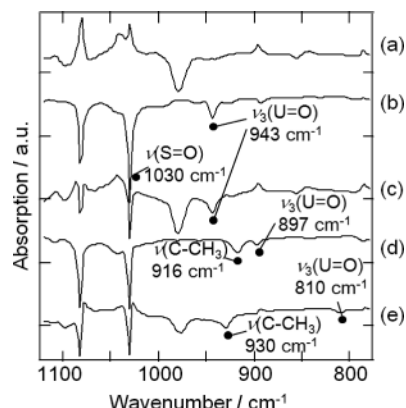


Figure 4. IR spectra of toluene solutions containing (a) $\text{B}(\text{C}_6\text{F}_5)_2\text{OH}$ ($2.5 \times 10^{-3} \text{ M}$), (b) $\text{UO}_2(\text{dfh})_2\text{DMSO}$ ($1.0 \times 10^{-3} \text{ M}$), (c) $\text{B}(\text{C}_6\text{F}_5)_2\text{OH}$ ($2.5 \times 10^{-3} \text{ M}$) and $\text{UO}_2(\text{dfh})_2\text{DMSO}$ ($1.0 \times 10^{-3} \text{ M}$), (d) $\text{UO}_2(\text{acac})_2\text{DMSO}$ ($1.0 \times 10^{-3} \text{ M}$), and (e) $\text{B}(\text{C}_6\text{F}_5)_2\text{OH}$ ($2.5 \times 10^{-3} \text{ M}$) and $\text{UO}_2(\text{acac})_2\text{DMSO}$ ($1.0 \times 10^{-3} \text{ M}$).

toluene solutions containing only $\text{B}(\text{C}_6\text{F}_5)_2\text{OH}$ or $\text{UO}_2(\text{dfh})_2\text{DMSO}$ (Figure 4a,b). The corresponding IR spectra for the $\text{UO}_2(\text{acac})_2\text{DMSO}$ system are also shown in Figure 4d,e. As seen from Figure 4b,c, the asymmetric $\text{O}=\text{U}=\text{O}$ stretching band [$\nu_3(\text{U}=\text{O})$] of $\text{UO}_2(\text{dfh})_2\text{DMSO}$ is observed at 943 cm^{-1} regardless of the addition of $\text{B}(\text{C}_6\text{F}_5)_2\text{OH}$. This result indicates that $\text{B}(\text{C}_6\text{F}_5)_2\text{OH}$ does not interact with $\text{UO}_2(\text{dfh})_2\text{DMSO}$ in a toluene solution and supports the results of ^{11}B and ^{17}O NMR measurements. On the other hand, as seen from Figure 4d,e, the $\nu_3(\text{U}=\text{O})$ band of $\text{UO}_2(\text{acac})_2\text{DMSO}$ observed at 897 cm^{-1} is shifted to 810 cm^{-1} with the addition of $\text{B}(\text{C}_6\text{F}_5)_2\text{OH}$. This indicates that the $\text{B}(\text{C}_6\text{F}_5)_2\text{OH}$ molecule interacts with the “yl” oxygen atoms of $\text{UO}_2(\text{acac})_2\text{DMSO}$ and results in a reduction of the bond strength of $\text{U}=\text{O}$.

The IR stretching frequency (ν) of the $\text{U}=\text{O}$ bond can be approximated by Hooke's law as follows:

$$\nu \text{ (cm}^{-1}\text{)} = \frac{1}{2\pi c} \left[F_{\text{uo}} \left(\frac{M_{\text{u}} + M_{\text{o}}}{M_{\text{u}} M_{\text{o}}} \right) \right]^{1/2} \quad (1)$$

where c , F_{uo} , M_{u} , and M_{o} are the velocity of light, the force constant of the U=O bond, and the masses of uranium and oxygen, respectively. We estimated the F_{uo} values using the $\nu_3(\text{U=O})$ values. The F_{uo} values of $\text{UO}_2(\text{dfh})_2\text{DMSO}$, $\text{UO}_2(\text{acac})_2\text{DMSO}$, and the mixture system of $\text{UO}_2(\text{acac})_2\text{DMSO}$ and $\text{B}(\text{C}_6\text{F}_5)_2\text{OH}$ were obtained as 7.85, 7.85, 7.11, and 5.80 $\text{mdyn } \text{\AA}^{-1}$, respectively. As expected, the U=O bond strength became weak in the solution containing $\text{UO}_2(\text{acac})_2\text{DMSO}$ and $\text{B}(\text{C}_6\text{F}_5)_2\text{OH}$. Furthermore, plots of the F_{uo} values against the ^{17}O - δs values (Figure 5) were found

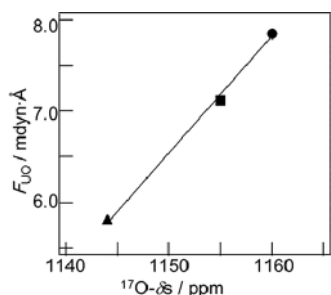


Figure 5. Plot of the force constant (F_{uo}) for the U=O bond versus ^{17}O NMR chemical shifts (^{17}O - δs): (●) $\text{UO}_2(\text{dfh})_2\text{DMSO}$ system, (■) $\text{UO}_2(\text{acac})_2\text{DMSO}$ system; (▲) the mixture system of $\text{UO}_2(\text{acac})_2\text{DMSO}$ and $\text{B}(\text{C}_6\text{F}_5)_2\text{OH}$.

to give a good linear relationship with a correlation coefficient of 0.997. This indicates that the change in the bond strength of

U=O is reflected in the ^{17}O - δs values, i.e., the electron density of the “yl” oxygen atom, and supports the results of ^{17}O NMR spectra shown in Figure 3 as being attributable to the LA–LB interaction between the boron atom of $\text{B}(\text{C}_6\text{F}_5)_2\text{OH}$ and the “yl” oxygen atom of $\text{UO}_2(\text{acac})_2\text{DMSO}$. Moreover, as seen from the IR spectrum (Figure 4e) for the system containing $\text{UO}_2(\text{acac})_2\text{DMSO}$ and $\text{B}(\text{C}_6\text{F}_5)_2\text{OH}$, the bands assigned to the C–CH₃ stretching [$\nu(\text{C–CH}_3)$] of acac shift from 916 to 930 cm^{-1} , and the S=O stretching band [$\nu(\text{S=O})$, 1030 cm^{-1}] of DMSO shows no shift.⁶⁰ This blue shift of $\nu(\text{C–CH}_3)$ is considered to be due to an increase of the coordination of acac to the uranyl moiety induced by the coordination of $\text{B}(\text{C}_6\text{F}_5)_2\text{OH}$ to the “yl” oxygen atoms of $\text{UO}_2(\text{acac})_2\text{DMSO}$, and no shift of $\nu(\text{S=O})$ indicates that the dissociation of DMSO from $\text{UO}_2(\text{acac})_2\text{DMSO}$ is not caused by the addition of $\text{B}(\text{C}_6\text{F}_5)_2\text{OH}$.

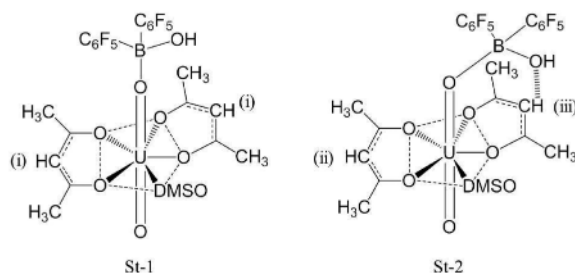
The results of IR measurements support the proposal derived from ^{11}B and ^{17}O NMR studies that the boron atom of $\text{B}(\text{C}_6\text{F}_5)_2\text{OH}$ interacts directly with the “yl” oxygen atom of $\text{UO}_2(\text{acac})_2\text{DMSO}$ in toluene, i.e., formation of the 1:1 and 2:1 complexes. From ^{11}B and ^{17}O NMR and IR data, it is proposed that the 1:1 and 2:1 complexes have St-1 and St-3 structures, respectively, as shown in Scheme 1.

On the basis of the viewpoints mentioned above, B···O=U bond formation should affect the proton and fluorine groups. Therefore, we measured ^{19}F and ^1H NMR spectra of toluene solutions containing $\text{B}(\text{C}_6\text{F}_5)_2\text{OH}$ and $\text{UO}_2(\text{dfh})_2\text{DMSO}$ or $\text{UO}_2(\text{acac})_2\text{DMSO}$ complexes.

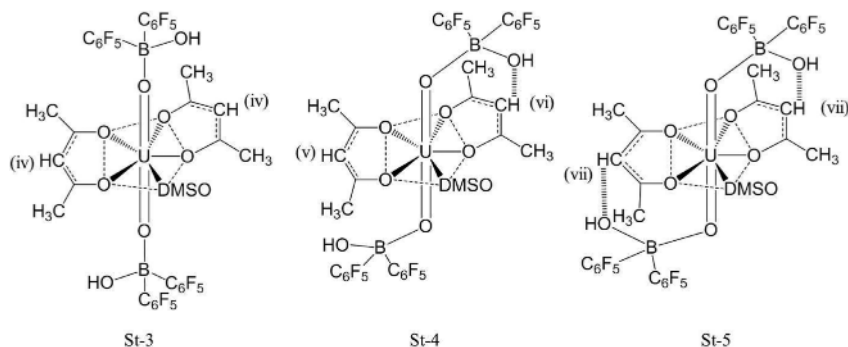
^{19}F NMR Spectra of Toluene Solutions Containing $\text{B}(\text{C}_6\text{F}_5)_2\text{OH}$ and Uranyl Complexes. ^{19}F NMR spectra of toluene solutions containing $\text{UO}_2(\text{dfh})_2\text{DMSO}$ (1.1×10^{-3} M) and $\text{B}(\text{C}_6\text{F}_5)_2\text{OH}$ [(0–1.1) $\times 10^{-3}$ M] were measured at

Scheme 1

1:1 LA-LB complexes



2:1 LA-LB complexes



25 °C. The results are shown in Figure S4 with the ^{19}F NMR spectrum of toluene solution dissolved in only $\text{B}(\text{C}_6\text{F}_5)_2\text{OH}$. The signals observed at -122.4 and -162.5 ppm in Figure S4a are assigned to the $-\text{CF}_3$ and $-\text{CF}_2$ groups of dfh in $\text{UO}_2(\text{dfh})_2\text{DMSO}$, respectively, and three signals (δ_{orig} : o , p , and m) at -133.1 , -148.2 , and -161.3 ppm in Figure S4b are assigned to the o -, p -, and m -fluorine atoms of the $-\text{C}_6\text{F}_5$ groups in $\text{B}(\text{C}_6\text{F}_5)_2\text{OH}$ on the basis of a previous paper.⁵⁴ In Figure S4, the chemical shifts and peak area ratios ($-\text{CF}_3$: $-\text{CF}_2$ = 1.5:1.0, o : p : m = 2:1:2) are almost constant, independent of $[\text{B}(\text{C}_6\text{F}_5)_2\text{OH}]_{\text{total}}$. This indicates that there are no specific interactions between the boron atom of $\text{B}(\text{C}_6\text{F}_5)_2\text{OH}$ and the fluorine atom of $\text{UO}_2(\text{dfh})_2\text{DMSO}$, as expected from ^{11}B and ^{17}O NMR studies.

On the other hand, ^{19}F NMR signals due to the $-\text{C}_6\text{F}_5$ group of $\text{B}(\text{C}_6\text{F}_5)_2\text{OH}$ in toluene solutions containing $\text{UO}_2(\text{acac})_2\text{DMSO}$ (1.0×10^{-3} M) and $\text{B}(\text{C}_6\text{F}_5)_2\text{OH}$ [(1.0–4.5) $\times 10^{-3}$ M] are found to be largely different from those in the $\text{UO}_2(\text{dfh})_2\text{DMSO}$ system, as shown in Figure 6. In Figure

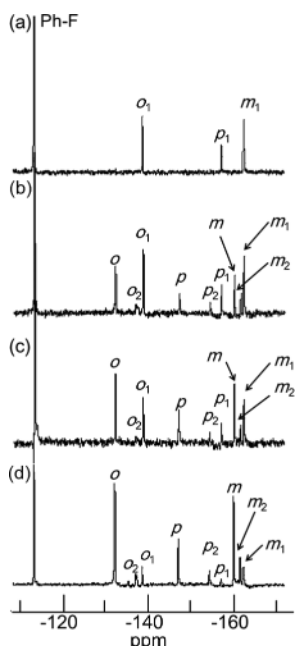


Figure 6. ^{19}F NMR spectra of toluene solutions containing $\text{B}(\text{C}_6\text{F}_5)_2\text{OH}$ and $\text{UO}_2(\text{acac})_2\text{DMSO}$ (1.1×10^{-3} M). $[\text{B}(\text{C}_6\text{F}_5)_2\text{OH}]_{\text{total}}$ = 1.0×10^{-3} M (a), 2.2×10^{-3} M (b), 2.8×10^{-3} M (c), and 4.5×10^{-3} M (d).

6a ($[\text{B}(\text{C}_6\text{F}_5)_2\text{OH}]_{\text{total}}$ = 1.0×10^{-3} M and $[\text{UO}_2(\text{acac})_2\text{DMSO}]$ = 1.0×10^{-3} M), three signals (δ_{new1} : o_1 , p_1 , m_1) are observed at around -139.7 , -158.2 , and -163.4 ppm, which are at higher magnetic fields than the signals (δ_{orig} : o , p , and m) shown in Figure S4b. The difference ($\Delta\delta_{m,p}$) in the chemical shifts of m - and p -fluorine atoms is known to be quite sensitive to changes in the environment of the boron atoms and the strength of LA–LB interactions.^{37,38,61,62} The $\Delta\delta_{m,p}$ values in Figures S4b and 6a are 13.1 and 5.2 ppm, respectively. These results suggest that the signals (δ_{new1} : o_1 , p_1 , m_1) in Figure 6a are assigned to the $-\text{C}_6\text{F}_5$ groups of $\text{B}(\text{C}_6\text{F}_5)_2\text{OH}$ coordinated to the “yl” oxygen atoms of $\text{UO}_2(\text{acac})_2\text{DMSO}$, i.e., formation of the 1:1 complex. After almost 2 equiv of $\text{B}(\text{C}_6\text{F}_5)_2\text{OH}$ (2.2×10^{-3} M) was added to $\text{UO}_2(\text{acac})_2\text{DMSO}$ (1.0×10^{-3} M), new signals (δ_{new2} : o_2 , p_2 ,

m_2) were observed at -138.1 , -155.5 , and -162.7 ppm with the δ_{orig} (o , p , and m) and δ_{new1} (o_1 , p_1 , and m_1) signals (Figure 6b). Furthermore, the intensities of the δ_{orig} and δ_{new2} signals are found to become larger than that of the δ_{new1} signal with increasing $[\text{B}(\text{C}_6\text{F}_5)_2\text{OH}]_{\text{total}}$. These results suggest that a species other than the 1:1 complex is formed and its fraction increases with an increase in $[\text{B}(\text{C}_6\text{F}_5)_2\text{OH}]_{\text{total}}$. The formed species is presumed to be the 2:1 complex and to be in equilibrium with the 1:1 complex.

In order to confirm the above equilibrium, the temperature dependence of the ^{19}F NMR spectra of toluene solutions containing $\text{UO}_2(\text{acac})_2\text{DMSO}$ (1.0×10^{-3} M) and $\text{B}(\text{C}_6\text{F}_5)_2\text{OH}$ ((0.5–4.5) $\times 10^{-3}$ M) was examined in the range of -30 to $+25$ °C. In the system of $[\text{B}(\text{C}_6\text{F}_5)_2\text{OH}]_{\text{total}}$ = (0.5–1.0) $\times 10^{-3}$ M and $[\text{UO}_2(\text{acac})_2\text{DMSO}]$ = 1.0×10^{-3} M, the peak areas of the δ_{new1} signals were almost constant, independent of temperature (e.g., see Figure S5). In the system of $[\text{B}(\text{C}_6\text{F}_5)_2\text{OH}]_{\text{total}}$ = 2.2×10^{-3} M and $[\text{UO}_2(\text{acac})_2\text{DMSO}]$ = 1.0×10^{-3} M, the peak intensities of the δ_{new1} and δ_{new2} signals decreased and increased, respectively, with decreasing temperature (Figure 7). Furthermore, in the system of

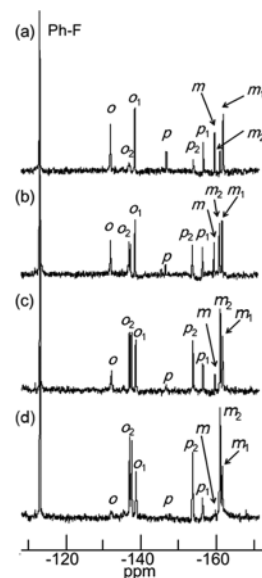
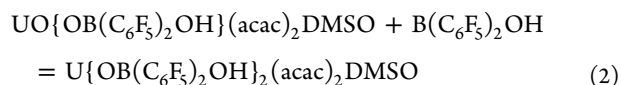


Figure 7. ^{19}F NMR spectra of toluene solutions containing $\text{B}(\text{C}_6\text{F}_5)_2\text{OH}$ (2.2×10^{-3} M) and $\text{UO}_2(\text{acac})_2\text{DMSO}$ (1.1×10^{-3} M) measured at $+25$ °C (a), 0 °C (b), -15 °C (c), and -30 °C (d).

$\text{B}(\text{C}_6\text{F}_5)_2\text{OH}$ = 4.5×10^{-3} M and $[\text{UO}_2(\text{acac})_2\text{DMSO}]$ = 1.0×10^{-3} M, the δ_{new1} peaks completely disappeared at -30 °C (Figure S6). These results indicate that the 1:1 and 2:1 complexes with the St-1 and St-3 structures shown in Scheme 1 exist in equilibrium in toluene solution as follows:



To evaluate the equilibrium constant (K), the peak areas of δ_{orig} , δ_{new1} , and δ_{new2} corresponding to the o -, p -, and m -fluorine atoms in Figure 7 were estimated by using the signal intensity of fluorobenzene (Ph-F, -113.0 ppm) as a reference and converted to the concentrations of $\text{B}(\text{C}_6\text{F}_5)_2\text{OH}$, $\text{UO}\{\text{OB}(\text{C}_6\text{F}_5)_2\text{OH}\}(\text{acac})_2\text{DMSO}$, and $\text{U}\{\text{OB}(\text{C}_6\text{F}_5)_2\text{OH}\}_2(\text{acac})_2\text{DMSO}$, respectively (abbreviated as

Table 1. Equilibrium Constant (K) at Various Temperatures for Toluene Solutions with Dissolved $\text{B}(\text{C}_6\text{F}_5)_2\text{OH}$ (2.2×10^{-3} or 2.8×10^{-3} M) and $\text{UO}_2(\text{acac})_2\text{DMSO}$ (1.0×10^{-3} M)

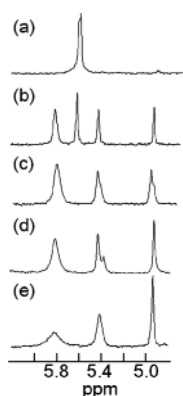
$[\text{B}(\text{C}_6\text{F}_5)_2\text{OH}]_{\text{total}}/\text{M}$	K/M^{-1}			
	25 °C	0 °C	−15 °C	−30 °C
2.2×10^{-3}	$(2.0 \pm 0.3) \times 10^2$	$(1.4 \pm 0.3) \times 10^3$	$(5.0 \pm 1.5) \times 10^3$	$(1.1 \pm 0.7) \times 10^4$
2.8×10^{-3}	$(3.1 \pm 0.6) \times 10^2$	$(9.0 \pm 0.8) \times 10^2$	$(2.5 \pm 0.7) \times 10^3$	$(1.5 \pm 0.5) \times 10^4$

$[\delta_{\text{orig}}]$, $[\delta_{\text{new1}}]$, and $[\delta_{\text{new2}}]$). The K values were calculated by the following relationship:

$$K = ([\delta_{\text{new2}}]/2)/([\delta_{\text{orig}}][\delta_{\text{new1}}]) \quad (3)$$

Similarly, the K values for the system of $[\text{B}(\text{C}_6\text{F}_5)_2\text{OH}]_{\text{total}} = 2.8 \times 10^{-3}$ M and $[\text{UO}_2(\text{acac})_2\text{DMSO}] = 1.0 \times 10^{-3}$ M were also obtained at each temperature. The results are listed in Table 1. In order to evaluate the thermodynamic parameters (ΔH and ΔS), the $\ln K$ values were plotted against the reciprocal temperature (Figure S7). The ΔH and ΔS values were obtained as -43.3 ± 4.9 kJ mol $^{-1}$ and -99.9 ± 18.3 J mol $^{-1}$ K $^{-1}$ for the system of $[\text{B}(\text{C}_6\text{F}_5)_2\text{OH}]_{\text{total}} = 2.2 \times 10^{-3}$ M and -41.5 ± 5.5 kJ mol $^{-1}$ and -93.4 ± 20.5 J mol $^{-1}$ K $^{-1}$ for the system of $[\text{B}(\text{C}_6\text{F}_5)_2\text{OH}]_{\text{total}} = 2.8 \times 10^{-3}$ M, respectively. The average ΔH and ΔS values were determined as -42.4 ± 5.2 kJ mol $^{-1}$ and -96.7 ± 19.4 J K $^{-1}$ mol $^{-1}$, respectively. The ΔG values in the temperature range of +25 to −30 °C are negative (−13.6 to −18.9 kJ mol $^{-1}$) and indicate that the 2:1 complex is thermodynamically more favorable.

^1H NMR Spectra of Toluene Solutions Containing $\text{B}(\text{C}_6\text{F}_5)_2\text{OH}$ and Uranyl Complexes. The behavior of the ^1H NMR signals of the $-\text{CH}$ groups of acac in $\text{UO}_2(\text{acac})_2\text{DMSO}$ were examined because the $-\text{CH}_3$ signals due to acac and DMSO overlap with that of toluene (Figure S8). The ^1H NMR spectra around 5.6 ppm of toluene solutions containing $\text{UO}_2(\text{acac})_2\text{DMSO}$ (1.0×10^{-3} M) and $\text{B}(\text{C}_6\text{F}_5)_2\text{OH}$ $[(0-5.0) \times 10^{-3}$ M] measured at 25 °C are shown in Figure 8. In Figure 8b ($[\text{B}(\text{C}_6\text{F}_5)_2\text{OH}]_{\text{total}}/$

**Figure 8.** ^1H NMR spectra of toluene solutions containing $\text{B}(\text{C}_6\text{F}_5)_2\text{OH}$ and $\text{UO}_2(\text{acac})_2\text{DMSO}$ (1.0×10^{-3} M) measured at 25 °C. $[\text{B}(\text{C}_6\text{F}_5)_2\text{OH}]_{\text{total}} = 0.0$ M (a), 5.0×10^{-3} M (b), 1.0×10^{-3} M (c), 2.5×10^{-3} M (d), and 5.0×10^{-3} M (e).

($[\text{UO}_2(\text{acac})_2\text{DMSO}] = 0.5$), three new signals are observed at 4.93, 5.42, and 5.80 ppm other than the $-\text{CH}$ signal (5.61 ppm; Figure 8a; $[\text{B}(\text{C}_6\text{F}_5)_2\text{OH}]_{\text{total}} = 0.0$ M) observed in the solution containing only $\text{UO}_2(\text{acac})_2\text{DMSO}$. In the solution of $[\text{B}(\text{C}_6\text{F}_5)_2\text{OH}]_{\text{total}}/([\text{UO}_2(\text{acac})_2\text{DMSO}] = 1.0$, the signal at 5.61 ppm disappears, as shown in Figure 8c. From ^{11}B and ^{17}O NMR studies, the 1:1 complex with the St-1 structure should

be formed under conditions of $[\text{B}(\text{C}_6\text{F}_5)_2\text{OH}]_{\text{total}}/[\text{UO}_2(\text{acac})_2\text{DMSO}] \leq 1$. If only the 1:1 complex with the St-1 symmetric structure is formed, the ^1H NMR signal at 5.61 ppm should shift to lower magnetic fields and give one signal related with the $-\text{CH}$ groups because formation of the St-1 structure generates a reduction of the electron density of acac of $\text{UO}_2(\text{acac})_2\text{DMSO}$. Hence, the new peak at 5.80 ppm is assigned as $-\text{CH}$ groups (i) of the St-1 structure. However, as shown in Figure 8b,c, two new peaks are observed at 4.93 and 5.42 ppm at a higher magnetic field than 5.61 ppm and the peak area ratios of the two signals are almost 1:1. These phenomena suggest that the 1:1 complex with a structure other than St-1 is formed under the condition $[\text{B}(\text{C}_6\text{F}_5)_2\text{OH}]_{\text{total}}/[\text{UO}_2(\text{acac})_2\text{DMSO}] \leq 1$. Therefore, we propose a St-2 asymmetric structure, shown in Scheme 1, as another 1:1 complex. In St-2, two kinds of $-\text{CH}$ groups of acac exist, i.e., one is $-\text{CH}$ interacting with the OH group of $\text{B}(\text{C}_6\text{F}_5)_2\text{OH}$ (iii) and another is noninteracting $-\text{CH}$ (ii). Because the electron density of acac of $\text{UO}_2(\text{acac})_2\text{DMSO}$ is enhanced by interactions with the OH group of $\text{B}(\text{C}_6\text{F}_5)_2\text{OH}$, the peaks of $-\text{CH}$ interacting with OH (iii in St-2) and noninteracting with $-\text{CH}$ (ii in St-2) should be observed at higher magnetic field regions (4.93 and 5.42 ppm) than the $-\text{CH}$ signal (5.61 ppm) of free $\text{UO}_2(\text{acac})_2\text{DMSO}$, respectively. It is thus indicated that three signals observed at 5.80, 5.42, and 4.93 ppm are assigned as the $-\text{CH}$ group (i) in St-1 and the $-\text{CH}$ groups (ii and iii) in St-2, respectively. Moreover, the three signals are found to drastically change with a further increase in $[\text{B}(\text{C}_6\text{F}_5)_2\text{OH}]_{\text{total}} [(2.5-5.0) \times 10^{-3}$ M], as shown in Figure 8d,e. This is considered to be due to formation of the 2:1 complex because, under the present conditions (2.5 and 5.0×10^{-3} M), the ratios of the 2:1 complex are estimated to be about 25 and 51%, respectively, by using the K value determined from the ^{19}F NMR spectra in Figure 7. From their similarity to the structure of the 1:1 complex, the complexes with St-4 and St-5 structures shown in Scheme 1 are proposed as a 2:1 complex other than St-3. Hence, the signals at around 5.8, 5.4, and 4.9 ppm may be assigned to the $-\text{CH}$ group (iv) in St-3, the $-\text{CH}$ groups (v and vi) in St-4, and the $-\text{CH}$ group (vii) in St-5, respectively; that is, the $-\text{CH}$ groups (I and iv) in St-1 and St-3, $-\text{CH}$ groups (ii and v) in St-2 and St-4, and $-\text{CH}$ groups (iii, vi, and vii) in St-2, St-4, and St-5 are expected to be observed at nearly the same chemical shifts.

In order to confirm the validity of the above proposal, the temperature dependence of the ^1H NMR spectra of toluene solutions containing $\text{UO}_2(\text{acac})_2\text{DMSO}$ (1.0×10^{-3} M) and $[\text{B}(\text{C}_6\text{F}_5)_2\text{OH}]_{\text{total}}$ (2.5×10^{-3} M) were examined in the range of −30 to +25 °C because in this solution the ratio of the 2:1 complex should increase with decreasing temperature on the basis of the K values (Table 1). The results are shown in Figures S9 and S10. It is found from Figure S10 that the signal intensity around 4.9 ppm increases relatively, that the signal around 5.8 ppm becomes broad and splits into two small peaks, that two signals around 5.3 ppm change their relative intensities, and that a new signal appears at around 8.0 ppm

and increases its intensity. These phenomena can be explained by the coexistence of 1:1 and 2:1 complexes. An increase in the intensity of the signal observed in the higher field of two signals around 5.3 ppm with decreasing temperature is considered to be because of the increase in the ratio of the 2:1 complex with decreasing temperature. On the basis of this viewpoint, the ratios of the 1:1 and 2:1 complexes were estimated from the peak area ratios of the two signals around 5.3 ppm. The results are 82:18, 47:53, 28:73, and 12:88 at +25, 0, −15, and −30 °C, respectively, and are almost consistent with those (72:28, 46:54, 32:68, 20:80) obtained from ^{19}F NMR measurements (Figure 7). Also, an increase in the relative intensity of the peak at around 4.8 ppm is thought to be attributable to an increase in the ratio of the 2:1 complex with the St-5 structure. From this point of view, the peak around 8.0 ppm is assigned to the −OH groups interacting with the −CH groups of coordinated acac because the −CH group of $\text{B}(\text{C}_6\text{F}_5)_2\text{OH}$ without any interaction with the LB compound is observed around 7.4 ppm.⁶² Furthermore, the decrease in the intensities of the peaks at around 5.8 ppm is supposed to be attributable to the decreases in the ratios of complexes with St-1 and St-3 structures.

The results of ^1H NMR measurements demonstrate that the LA–LB complexes consisting of $\text{B}(\text{C}_6\text{F}_5)_2\text{OH}$ and $\text{UO}_2(\text{acac})_2\text{DMSO}$ in toluene have some coordination geometries (St-1–St-5) and their ratios change depending on $[\text{B}(\text{C}_6\text{F}_5)_2\text{OH}]_{\text{total}}$ and temperatures.

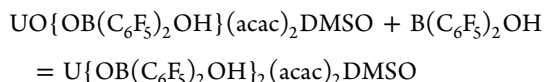
CONCLUSION

In order to clarify the LA–LB complexation processes between the boron atom of $\text{B}(\text{C}_6\text{F}_5)_2\text{OH}$ and the “yl” oxygen atoms of uranyl β -diketonato complexes, we investigated ^1H , ^{11}B , ^{17}O , and ^{19}F NMR and IR spectra of toluene solutions containing β -diketonato complexes [$\text{UO}_2(\text{dfh})_2\text{DMSO}$ or $\text{UO}_2(\text{acac})_2\text{DMSO}$] and $\text{B}(\text{C}_6\text{F}_5)_2\text{OH}$. The results are summarized as follows.

(a) Interaction between the boron atom of $\text{B}(\text{C}_6\text{F}_5)_2\text{OH}$ and the “yl” oxygen atom of $\text{UO}_2(\text{dfh})_2\text{DMSO}$ does not occur in toluene. This is attributable to the weak donicity of the “yl” oxygen atom of $\text{UO}_2(\text{dfh})_2\text{DMSO}$ with dfh having electro-negative $-\text{C}_2\text{F}_5$ groups.

(b) The “yl” oxygen atoms of $\text{UO}_2(\text{acac})_2\text{DMSO}$ interact with the boron atom of $\text{B}(\text{C}_6\text{F}_5)_2\text{OH}$ in toluene. Under the conditions $[\text{B}(\text{C}_6\text{F}_5)_2\text{OH}]_{\text{total}}/[\text{UO}_2(\text{acac})_2\text{DMSO}] \leq 1$, the 1:1 LA–LB complex can be formed stoichiometrically.

(c) Under the conditions, $[\text{B}(\text{C}_6\text{F}_5)_2\text{OH}]_{\text{total}}/[\text{UO}_2(\text{acac})_2\text{DMSO}] > 1$, the 2:1 LA–LB complex is formed and exists in equilibrium with the 1:1 complex in toluene as follows:



(d) The thermodynamic parameters, K , ΔH , and ΔS , were determined to be $(2.5 \pm 0.6) \times 10^2 \text{ M}^{-1}$, $-42.4 \pm 5.2 \text{ kJ mol}^{-1}$, and $-96.7 \pm 19.4 \text{ J K}^{-1} \text{ mol}^{-1}$, respectively.

(e) Two kinds of 1:1 complexes are formed; i.e., one is the complex with bonding between the −OH group of $\text{B}(\text{C}_6\text{F}_5)_2\text{OH}$ and the −CH group of acac ($\text{CH}\cdots\text{OH}$ bond), and another is the complex without such bonding.

(f) Three kinds of 2:1 complexes are formed, i.e., one without a $\text{CH}\cdots\text{OH}$ bond, another with one $\text{CH}\cdots\text{OH}$ bond, and the third with two $\text{CH}\cdots\text{OH}$ bonds.

(g) Finally, it is concluded that the “yl” oxygen atom of uranyl complexes with β -diketonato possessing weak electro-negative groups can form an LA–LB complex.

ASSOCIATED CONTENT

Supporting Information

The Supporting Information is available free of charge at <https://pubs.acs.org/doi/10.1021/acs.inorgchem.0c00979>.

^1H , ^{11}B , and ^{19}F NMR spectra and plots of $\ln K$ versus reciprocal temperature (PDF)

AUTHOR INFORMATION

Corresponding Author

Takehiko Tsukahara – Laboratory for Advanced Nuclear Energy, Institute of Innovative Research, Tokyo Institute of Technology, Meguro-ku, Tokyo 152-8550, Japan; orcid.org/0000-0001-9395-5516; Phone: +81-3-5734-3067; Email: ptsuka@lane.iir.titech.ac.jp; Fax: +81-3-5734-3067

Authors

Naomi Miyamoto – Laboratory for Advanced Nuclear Energy, Institute of Innovative Research, Tokyo Institute of Technology, Meguro-ku, Tokyo 152-8550, Japan

Yasuhisa Ikeda – Laboratory for Advanced Nuclear Energy, Institute of Innovative Research, Tokyo Institute of Technology, Meguro-ku, Tokyo 152-8550, Japan

Complete contact information is available at:

<https://pubs.acs.org/doi/10.1021/acs.inorgchem.0c00979>

Notes

The authors declare no competing financial interest.

REFERENCES

- (1) Denning, R. G. Electronic Structure and Bonding in Actinyl Ions and their Analogs. *J. Phys. Chem. A* **2007**, *111*, 4125–4143.
- (2) Limberg, C. On the Trail of CrO_2Cl_2 in Its Reactions with Organic Compounds. *Chem. - Eur. J.* **2000**, *6*, 2083–2089.
- (3) Limberg, C. The Role of Radicals in Metal-Assisted Oxygenation Reactions. *Angew. Chem., Int. Ed.* **2003**, *42*, 5932–5954.
- (4) Arnold, P. L.; Love, J. B.; Patel, D. Pentavalent uranyl complexes. *Coord. Chem. Rev.* **2009**, *253*, 1973–1978.
- (5) Amme, M.; Wiss, T.; Thiele, H.; Boulet, P.; Lang, H. Uranium secondary phase formation during anoxic hydrothermal leaching processes of UO_2 nuclear fuel. *J. Nucl. Mater.* **2005**, *341*, 209–223.
- (6) Delemos, J. L.; Bostick, B. C.; Quicksall, A. N.; Landis, J. D.; George, C. C.; Slagowski, N. L.; Rock, T.; Brugge, D.; Lewis, J.; Durant, J. L. Rapid dissolution of soluble uranyl phases in arid, mine-impacted catchments near Church Rock, NM. *Environ. Sci. Technol.* **2008**, *42*, 3951–3957.
- (7) Fortier, S.; Hayton, T. W. Oxo ligand functionalization in the uranyl ion (UO_2^{2+}). *Coord. Chem. Rev.* **2010**, *254*, 197–214.
- (8) Arnold, P. L.; Pécharman, A.; Hollis, E.; Yahia, A.; Maron, L.; Parsons, S.; Love, J. B. Uranyl oxo activation and functionalization by metal cation coordination. *Nat. Chem.* **2010**, *2*, 1056–1061.
- (9) Coughlin, E. J.; Qiao, Y.; Lapsheva, R.; Zeller, M.; Schelter, E. J.; Bart, S. C. Uranyl Functionalization Mediated by Redox-Active Ligands: Generation of O–C Bonds via Acylation. *J. Am. Chem. Soc.* **2019**, *141*, 1016–1026.
- (10) Cowie, B. E.; Purkis, J. M.; Austin, J.; Love, J. B.; Arnold, P. L. Thermal and Photochemical Reduction and Functionalization Chemistry of the Uranyl Dication, $[\text{U}^{\text{VI}}\text{O}_2]^{2+}$. *Chem. Rev.* **2019**, *119*, 10595–10637.
- (11) Clark, D. L.; Conradson, S. D.; Donohoe, R. J.; Keogh, D. W.; Morris, D. E.; Palmer, P. D.; Rogers, R. D.; Tait, C. D. Chemical Speciation of the Uranyl Ion under Highly Alkaline Conditions.

Synthesis, Structures, and Oxo Ligand Exchange Dynamics. *Inorg. Chem.* **1999**, *38*, 1456–1466.

(12) Szabó, Z.; Grenthe, I. Reactivity of the “yl”-Bond in Uranyl(VI) Complexes. 1. Rates and Mechanisms for the Exchange between the trans-dioxo Oxygen Atoms in $(\text{UO}_2)_2(\text{OH})_2^{2+}$ and Mononuclear $\text{UO}_2(\text{OH})_n^{2-n}$ Complexes with Solvent Water. *Inorg. Chem.* **2007**, *46*, 9372–9378.

(13) Réal, F.; Vallet, V.; Wahlgren, U.; Grenthe, I. Ab Initio Study of the Mechanism for Photoinduced Yl-Oxygen Exchange in Uranyl(VI) in Acidic Aqueous Solution. *J. Am. Chem. Soc.* **2008**, *130*, 11742–11751.

(14) Rios, D.; del Carmen Michelini, M.; Lucena, A. F.; Marçalo, J.; Gibson, J. K. On the Origins of Faster Oxo Exchange for Uranyl(V) versus Plutonyl(V). *J. Am. Chem. Soc.* **2012**, *134*, 15488–15496.

(15) Tsushima, S. yl[−]-Oxygen Exchange in Uranyl(VI) Ion: A Mechanism Involving $(\text{UO}_2)_2(\mu\text{-OH})_2^{2+}$ via U–Oyl–U Bridge Formation. *Inorg. Chem.* **2012**, *51*, 1434–1439.

(16) Brown, D. R.; Denning, R. G. Stable Analogs of the Uranyl Ion Containing the -NUN- Group. *Inorg. Chem.* **1996**, *35*, 6158–6163.

(17) Duval, P. B.; Burns, C. J.; Buschmann, W. E.; Clark, D. L.; Morris, D. E.; Scott, B. L. Reaction of the Uranyl(VI) Ion (UO_2^{2+}) with a Triamidoamine Ligand: Preparation and Structural Characterization of a Mixed-Valent Uranium(V/VI) Oxo-Imido Dimer. *Inorg. Chem.* **2001**, *40*, 5491–5496.

(18) Wahlgren, U.; Moll, H.; Grenthe, I.; Schimmelpfennig, B.; Maron, L.; Vallet, V.; Groen, O. Structure of Uranium(VI) in Strong Alkaline Solutions. A Combined Theoretical and Experimental Investigation. *J. Phys. Chem. A* **1999**, *103*, 8257–8264.

(19) Wilkerson, M. P.; Burns, C. J.; Dewey, H. J.; Martin, J. M.; Morris, D. E.; Paine, R. T.; Scott, B. L. Basicity of Uranyl Oxo Ligands upon Coordination of Alkoxides. *Inorg. Chem.* **2000**, *39*, 5277–5285.

(20) Baker, R. J. New Reactivity of the Uranyl(VI) Ion. *Chem. - Eur. J.* **2012**, *18*, 16258–16271.

(21) Pedrick, E. A.; Wu, G.; Hayton, T. W. Oxo Ligand Substitution in a Cationic Uranyl Complex: Synergistic Interaction of an Electrophile and a Reductant. *Inorg. Chem.* **2015**, *54*, 7038–7044.

(22) Arnold, P. L.; Patel, D.; Wilson, C.; Love, J. B. Reduction and selective oxo group silylation of the uranyl dication. *Nature* **2008**, *451*, 315–318.

(23) Schnaars, D. D.; Wu, G.; Hayton, T. W. Silylation of the Uranyl Ion Using $\text{B}(\text{C}_6\text{F}_5)_3$ -Activated Et_3SiH . *Inorg. Chem.* **2011**, *50*, 9642–9649.

(24) Natrajan, L.; Burdet, F.; Pécaut, J.; Mazzanti, M. Synthesis and Structure of a Stable Pentavalent-Uranyl Coordination Polymer. *J. Am. Chem. Soc.* **2006**, *128*, 7152–7153.

(25) Berthet, J.-C.; Siffredi, G.; Thuéry, P.; Ephritikhine, M. Synthesis and crystal structure of pentavalent uranyl complexes. The remarkable stability of UO_2X ($\text{X} = \text{I}, \text{SO}_3\text{CF}_3$) in non-aqueous solutions. *Dalton. Trans.* **2009**, *18*, 3478–3494.

(26) Burdet, F.; Pécaut, J.; Mazzanti, M. Isolation of a Tetrameric Cation-Cation Complex of Pentavalent Uranyl. *J. Am. Chem. Soc.* **2006**, *128*, 16512–16513.

(27) Nocton, G.; Horeglad, P.; Pécaut, M.; Mazzanti, M. Polynuclear Cation-Cation Complexes of Pentavalent Uranyl: Relating Stability and Magnetic Properties to Structure. *J. Am. Chem. Soc.* **2008**, *130*, 16633–16634.

(28) Nocton, G.; Horeglad, P.; Vetere, V.; Pécaut, J.; Dubois, L.; Maldivi, P.; Edelstein, N. M.; Mazzanti, M. Synthesis, Structure, and Bonding of Stable Complexes of Pentavalent Uranyl. *J. Am. Chem. Soc.* **2010**, *132*, 495–496.

(29) Arnold, P. L.; Patel, D.; Blake, A. J.; Wilson, C.; Love, J. B. Selective Oxo Functionalization of the Uranyl Ion with 3d Metal Cations. *J. Am. Chem. Soc.* **2006**, *128*, 9610–9611.

(30) Arnold, P. L.; Hollis, E.; White, F. J.; Magnani, N.; Caciuffo, R.; Love, J. B. Single-Electron Uranyl Reduction by a Rare-Earth Cation. *Angew. Chem.* **2011**, *123*, 917–920.

(31) Bell, N. L.; Arnold, P. L.; Love, J. B. Controlling uranyl oxo group interactions to group 14 elements using polypyrrolic Schiff-base macrocyclic ligands. *Dalton Trans.* **2016**, *45*, 15902–15909.

(32) Pattenau, S. A.; Coughlin, E. J.; Collins, T. S.; Zeller, M.; Bart, S. C. Expanding the Library of Uranyl Amide Derivatives: New Complexes Featuring the tert-Butyldimethylsilylamide Ligand. *Inorg. Chem.* **2018**, *57*, 4543–4549.

(33) Sarsfield, M. J.; Helliwell, M. Extending the Chemistry of the Uranyl Ion: Lewis Acid Coordination to a $\text{U}=\text{O}$ Oxygen. *J. Am. Chem. Soc.* **2004**, *126*, 1036–1037.

(34) Hayton, T. W.; Wu, G. Exploring the Effects of Reduction or Lewis Acid Coordination on the $\text{U}=\text{O}$ Bond of the Uranyl Moiety. *Inorg. Chem.* **2009**, *48*, 3065–3072.

(35) Schnaars, D. D.; Wu, G.; Hayton, T. W. Reduction of Pentavalent Uranyl to U(IV) Facilitated by Oxo Functionalization. *J. Am. Chem. Soc.* **2009**, *131*, 17532–17533.

(36) Sarsfield, M. J.; Helliwell, M.; Raftery, J. Distorted Equatorial Coordination Environments and Weakening of UO Bonds in Uranyl Complexes Containing NCN and NPN Ligands. *Inorg. Chem.* **2004**, *43*, 3170–3179.

(37) Piers, W. E. The chemistry of perfluoroaryl boranes. *Adv. Organomet. Chem.* **2004**, *52*, 1–76.

(38) Beringhelli, T.; Maggioni, D.; D'Alfonso, G. ^1H and ^{19}F NMR Investigation of the Reaction of $\text{B}(\text{C}_6\text{F}_5)_3$ with Water in Toluene Solution. *Organometallics* **2001**, *20*, 4927–4938.

(39) Ikeda, Y.; Tomiyasu, H.; Fukutomi, H. Nuclear magnetic resonance study of the kinetics of ligand-exchange reactions in uranyl complexes. 5. Exchange reaction of acetylacetonate in bis-(acetylacetonato)(dimethyl sulfoxide)dioxouranium(VI). *Inorg. Chem.* **1984**, *23*, 3197–3201.

(40) Jung, W. S.; Ikeda, Y.; Tomiyasu, H.; Fukutomi, H. Oxygen Isotope Shifts in ^{17}O NMR Spectra of the Uranyl Ion. *Bull. Chem. Soc. Jpn.* **1984**, *57*, 2317–2318.

(41) Brucher, E.; Glaser, J.; Toth, I. Carbonate exchange for the complex tris(carbonato)dioxouranate(4[−]) in aqueous solution as studied by carbon-13-NMR spectroscopy. *Inorg. Chem.* **1991**, *30*, 2239–2241.

(42) Szabó, Z.; Glaser, J.; Grenthe, I. Kinetics of Ligand Exchange Reactions for Uranyl(2⁺) Fluoride Complexes in Aqueous Solution. *Inorg. Chem.* **1996**, *35*, 2036–2044.

(43) Hatakeyama, K.; Arai, K.; Harada, M.; Ikeda, Y.; Tomiyasu, H. A Nuclear Magnetic Resonance Study on Ligand Exchange Reaction in U(VI) Nitrate Complex with n-Octyl(phenyl)-N, N-Diisobutyl-carbamoylmethylphosphine Oxide in Acetone Containing Oxalic Acid. *J. Nucl. Sci. Technol.* **1997**, *34*, 1133–1139.

(44) Muntean, J. V.; Nash, K. L.; Rickert, P. G.; Sullivan, J. C. Dynamic NMR Study of Ligand Exchange Reactions in U(VI)-Phosphonic Acid Systems. *J. Phys. Chem. A* **1999**, *103*, 3383–3387.

(45) Jacopin, C.; Sawicki, M.; Plancque, G.; Doizi, D.; Taran, F.; Ansoborlo, E.; Amekraz, B.; Moulin, C. Investigation of the Interaction between 1-Hydroxyethane-1,1'-diphosphonic Acid (HEDP) and Uranium(VI). *Inorg. Chem.* **2003**, *42*, 5015–5022.

(46) Mizuoka, K.; Grenthe, I.; Ikeda, Y. Structural and Kinetic Studies on Uranyl(V) Carbonate Complex Using ^{13}C NMR Spectroscopy. *Inorg. Chem.* **2005**, *44*, 4472–4474.

(47) Tsukahara, T.; Kachi, Y.; Kayaki, Y.; Ikariya, T.; Ikeda, Y. ^1H , ^{13}C , and ^{19}F NMR Studies on Molecular Interactions of CO_2 with β -Diketones and $\text{UO}_2(\beta\text{-diketonato})_2$ DMSO Complexes in Supercritical CO_2 . *J. Phys. Chem. B* **2008**, *112*, 16445–16454.

(48) Takao, K.; Takahashi, T.; Ikeda, Y. Complex Formation of Uranyl Ion with Triphenylphosphine Oxide and Its Ligand Exchange Reaction in 1-Butyl-3-methylimidazolium Nonfluorobutanesulfonate Ionic Liquid. *Inorg. Chem.* **2009**, *48*, 1744–1752.

(49) Szabó, Z.; Grenthe, I. On the Mechanism of Oxygen Exchange Between Uranyl(VI) Oxygen and Water in Strongly Alkaline Solution as Studied by ^{17}O NMR Magnetization Transfer. *Inorg. Chem.* **2010**, *49*, 4928–4933.

(50) Marchenko, A.; Truandier, L. A.; Autschbach, J. Uranyl Carbonate Complexes in Aqueous Solution and Their Ligand NMR Chemical Shifts and ^{17}O Quadrupolar Relaxation Studied by ab Initio Molecular Dynamics. *Inorg. Chem.* **2017**, *56*, 7384–7396.

(51) Miyamoto, N.; Tsukahara, T.; Ikeda, Y. NMR Spectroscopic Evidence of Lewis Acid–Lewis Base Complex Formation of Perfluoroborane with Uranyl β -Diketonato Complexes. *Chem. Lett.* **2012**, *41*, 513–515.

(52) Mizuguchi, K.; Lee, S.-H.; Ikeda, Y.; Tomiyasu, H. Electrochemical studies on bis(β -diketonato)(dimethyl sulfoxide)-dioxouranium(VI) in dimethyl sulfoxide. *J. Alloys Compd.* **1998**, *271*–*273*, 163–167.

(53) Ikeno, I.; Mitsui, H.; Iida, T.; Moriguchi, T. U.S. Patent 6,818,785, 2004.

(54) Tian, J.; Wang, S.; Feng, Y.; Li, J.; Collins, S. Borane-functionalized oxide supports: development of active supported metallocene catalysts at low aluminoxane loading. *J. Mol. Catal. A: Chem.* **1999**, *144*, 137–150.

(55) Beringhelli, T.; Donghi, D.; Maggioni, D.; D'Alfonso, G. Solution structure, dynamics and speciation of perfluoroaryl boranes through ^1H , ^{11}B and ^{19}F NMR spectroscopy. *Coord. Chem. Rev.* **2008**, *252*, 2292–2313.

(56) Gordon, G.; Taube, H. The uranium(V)-catalysed exchange reaction between uranyl ion and water in perchloric acid solution. *J. Inorg. Nucl. Chem.* **1961**, *16*, 272–278.

(57) Miyamoto, N.; Tsukahara, T.; Kachi, Y.; Harada, M.; Kayaki, Y.; Ikariya, T.; Ikeda, Y. Studies on solubility of uranyl complexes in supercritical carbon dioxide and its controlling factors using UV-visible and ^{17}O - and ^{19}F -NMR spectroscopy. *J. Nucl. Sci. Technol.* **2012**, *49*, 37–46.

(58) Tsukahara, T.; Harada, M.; Ikeda, Y.; Tomiyasu, H. ^{17}O Chemical shift and spin-lattice relaxation measurements of water in liquid and supercritical states by using high-resolution multinuclear NMR. *J. Supercrit. Fluids* **2003**, *26*, 73–82.

(59) Galsworthy, J. R.; Green, M. L. H.; Muller, M.; Prout, K. Reactions of transition-metal oxo complexes with $\text{B}(\text{C}_6\text{F}_5)_3$: crystal structures of $[\text{V}\{\text{OB}(\text{C}_6\text{F}_5)_3\}(\text{acac})_2]$, $[\text{Ti}\{\text{OB}(\text{C}_6\text{F}_5)_3\}(\text{acac})_2]$ and $\text{cis-}[\text{MoO}\{\text{OB}(\text{C}_6\text{F}_5)_3\}(\text{acac})_2]$ (acac = acetylacetonate). *J. Chem. Soc., Dalton Trans.* **1997**, *8*, 1309–1313.

(60) Nakamoto, K.; Morimoto, Y.; Martell, A. E. Infrared Spectra of Metal Chelate Compounds. IV. Infrared Spectra of Addition Compounds of Metallic Acetylacetonates. *J. Am. Chem. Soc.* **1961**, *83*, 4533–4536.

(61) Beringhelli, T.; D'Alfonso, G.; Donghi, D.; Maggioni, D.; Mercandelli, P.; Sironi, A. The Role of Water in the Oligomerization Equilibria Involving Bis(pentafluorophenyl)borinic Acid in Dichloromethane Solution. *Organometallics* **2004**, *23*, 5493–5502.

(62) Donghi, D.; Maggioni, D.; Beringhelli, T.; D'Alfonso, G.; Mercandelli, P.; Sironi, A. Hydrogen Bonding and Lewis Acid–Base Interactions in the System Bis(pentafluorophenyl)borinic Acid/Methanol. *Eur. J. Inorg. Chem.* **2008**, *10*, 1645–1653.